Water Research 274 (2025) 123127

Contents lists available at ScienceDirect

Water Research

journal homepage: www.elsevier.com/locate/watres

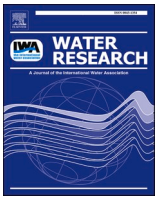

Polyelectrolyte nanofiltration membranes for base separation and recovery

Joshua L. Livingston [a], Abigail Cafferty [b], Riley Miller [a], Allison V. Cordova-Huaman [a], Jin Zhang [b], G. Kane Jennings [a], Shihong Lin [a,b,*]

[a] Department of Chemical and Biomolecular Engineering, Vanderbilt University, Nashville, TN 37205, USA
[b] Department of Civil and Environmental Engineering, Vanderbilt University, Nashville, TN 37205, USA

ARTICLE INFO

Keywords:
Nanofiltration
Polyelectrolyte membrane
Alkaline resistance
Hydroxide separation
Resource recovery

ABSTRACT

Nanofiltration (NF) membranes have the potential to significantly advance resource recovery efforts where monovalent/divalent ion separation is critical, but their utilization is limited by inadequate stability under extreme conditions. "Base separation"—i.e., separating hydroxide from other ions—has emerged as an essential approach in resource recovery, enabling the extraction of multivalent anions (e.g., carbonates and phosphates) from hydroxide-rich streams. There is a particularly high demand for membranes capable of separating carbonates from hydroxide-rich CO_2 capture solvents and phosphates from hydroxide-rich adsorbent regeneration solvents. However, conventional polyamide NF membranes degrade during long-term exposure to alkaline conditions, limiting their application in extreme conditions. In this study, alkaline-resistant polyelectrolyte membranes are fabricated by depositing alternating layers of polycation, poly(diallyl dimethylammonium chloride) (PDADMAC), and polyanion, poly(sodium 4-styrenesulfonate) (PSS) to a polyethersulfone substrate. The membranes are tested for hydroxide/carbonate and hydroxide/phosphate separation performance, as well as performance stability during prolonged exposure to highly alkaline conditions. Results indicate that higher feed solution pH improves carbonate and phosphate rejection by promoting ion deprotonation and strengthening electrostatic repulsion from the negatively charged membrane. In contrast, increasing carbonate and phosphate concentrations in the feed solution reduces the rejection due to charge screening. The six-bilayer PDADMAC/PSS membrane removes more than 99 % of carbonates and phosphates while allowing extensive passage of hydroxide at pH 13. Stability tests confirm that PDADMAC/PSS membranes maintain excellent ion selectivity over four weeks of exposure to pH 13 KOH, whereas commercial polyamide NF membranes degrade within one week. These findings highlight the potential for PDADMAC/PSS membranes to advance critical resource recovery efforts, providing a durable and effective solution for applications under extreme conditions.

1. Introduction

Base recovery processes are increasingly recognized as vital tools in resource recovery and sustainability. These processes generally aim to purify hydroxide streams by removing target species from spent hydroxide-rich solutions. Basic solutions are widely employed as cleaning agents due to the high solubility of OH^- in water and their effectiveness in dissolving chemical species when used as absorbent regenerants, cleaning agents, or leaching solutions (Gésan-Guiziou et al., 2007). Sustainable operation hinges critically on the regeneration of caustic solutions, highlighting the dual advantage of recycling – economic efficiency and reduced environmental footprint from the discharge or treatment of caustic solutions. Case studies investigating caustic recovery in various industries, including chitin production, dairy processing, the mercerization of cotton in the textile industry, and the recovery of hemicellulose from wheat bran and barley husks, have underscored the promise of membrane filtration processes in both removing dissolved species and concurrently purifying and recovering caustic solutions (Arkell et al., 2013; Merin et al., 2002; Zhao and Xia, 2009). These base recovery processes often involve complex mixtures of OH^-, suspended solids, organic matter, and salts.

In certain applications, the separation of OH^- from other anions serves as not only as a means of caustic solution recovery but also the purification and concentration of the anions as the product. For illustration, two such examples are provided here. One promising way to perform direct air CO_2 capture is to use hydroxide-rich solutions as environmentally friendly capture solvents (versus most amine-based solvents). The OH^- ions in solution react rapidly with CO_2 to form

* Corresponding author.
E-mail address: shihong.lin@Vanderbilt.edu (S. Lin).

https://doi.org/10.1016/j.watres.2025.123127
Received 8 October 2024; Received in revised form 24 December 2024; Accepted 9 January 2025
Available online 11 January 2025

water soluble carbonates. This reaction 'captures' CO_2 from the atmosphere and temporarily stores it in the capture solvent. The conventional method of regenerating KOH or NaOH capture solvents involves heating the solution to 800 °C to thermally decompose K_2CO_3 (Na_2CO_3) into K_2O (Na_2O), which reacts with water to generate KOH (NaOH) (Kar et al., 2018). Ideally, a OH^- separation process should more efficiently regenerate the capture solvent while concentrating the captured carbonates for further processing. In the second example, hydroxide separation is also essential for the recovery of phosphate from adsorbents. Phosphorus, an essential mineral for human health and key component of fertilizer, is primarily obtained from mining phosphate rock and thus considered an exhaustible resource (Cooper et al., 2011). Various processes have been developed to recover phosphorus from wastewater to mitigate eutrophication and promote resource circularity (Conley et al., 2009; Geissler et al., 2018). However, adsorption remains the most practical approach to recover phosphorus from a low concentration stream and reduce the effluent phosphorus concentration to below 5 mg L^{-1} (Geissler et al., 2018; Sena et al., 2021). Hydroxide-rich solutions are widely reported as the most effective adsorbent regenerants to release phosphate species at high pH (Sena et al., 2021). Similar to the CO_2 capture process, phosphate species must be recovered and concentrated for further treatment while the basic solution is ideally recycled and reused. Nanofiltration (NF) is a promising approach for base recovery, particularly for its ability to perform multivalent/monovalent ion separations. NF membranes have shown significant potential in applications such as water softening and lithium extraction from magnesium-rich brines (Labban et al., 2017; Li et al., 2023; Song et al., 2016; Wang et al., 2023). In the context of lithium-ion battery recycling, lithium can also be recovered by leaching spent cathodes with a concentrated base (Ferreira et al., 2009; Joshi et al., 2024; Su et al., 2024). An NF membrane capable of separating the leached cations from lithium, and recovering lithium as lithium hydroxide, could eliminate numerous costly steps in the typical lithium-ion battery recycling process (Su et al., 2024). However, base recovery efforts in lithium-ion battery recycling, direct air CO_2 capture, and phosphorus recovery from adsorbents face a common challenge: the lack of commercially available NF membranes that offer both strong ion-ion selectivity and long-term stability in caustic solutions.

Poly(piperazine-amide) membranes are the state-of-the-art NF membranes, offering high water permeance and outstanding separation performance. The poly(piperazine-amide) active layer is prepared using interfacial polymerization between piperazine and trimesoyl chloride. However, carbonyl carbons in polyamide bonds are electron deficient and susceptible to nucleophilic attack, rendering the polyamide active layer vulnerable to degradation outside of mild conditions ($3 \leq pH \leq 10$) (Huang et al., 2020; Ma et al., 2015; Paul and Jons, 2016; Yang et al., 2022). Ideally, NF membranes employed for base recovery should maintain performance stability during long-term exposure to alkaline conditions. Beyond alkaline stability, an ideal membrane for base recovery should have low OH^- rejection and high rejection to multivalent anions (e.g., CO_3^{2-} and PO_4^{3-}) to concentrate the CO_3^{2-} or PO_4^{3-} ions in the retentate and recover OH^- in the permeate to the greatest extent possible. Although not specifically tested for hydroxide separation, alkaline-resistant NF membranes have been developed in recent years. The replacement of trimesoyl chloride with cyanuric chloride in the organic phase during interfacial polymerization yields poly (s-triazine amine) NF membranes, which are stable in base for much longer time than are polyamide NF membranes (Bai et al., 2022; Lee et al., 2015; Lee et al., 2017). However, cyanuric chloride is less reactive than trimesoyl chloride, does not yield active layers with a high negative charge density optimal for base recovery separations, and is primarily targeted toward removal of multivalent cations from aqueous mixtures (Bai et al., 2022; Just et al., 1995; Thurston et al., 1951; Yu et al., 2020). Polyurea NF membranes are more promising for base recovery separations, featuring ultra-stable, negatively charged active layers capable of >90 % multivalent anion removal; however, their water permeabilities do not approach that of state-of-the-art NF membranes (Zhang et al., 2021; Zhang et al., 2022).

One promising approach for developing alkaline-resistant membranes is based on layer-by-layer (LbL) deposition of oppositely charged polyelectrolytes. In polyelectrolyte NF (PE-NF) membranes, the active layer is formed by the electrostatic attraction between polyanions and polycations, eliminating the reliance on covalent bonds that may degrade under extreme conditions. However, PE-NF membranes are not all inherently stable under extreme pH conditions. To achieve alkaline-resistance, a PE-NF membrane should comprise polycations and polyanions that retain their respective charge under alkaline conditions. Thus, alkaline-resistant NF membranes could be fabricated using oppositely charged strong polyelectrolytes (i.e., polyelectrolytes whose degree of ionization are independent of pH). Poly(diallyldimethylammonium chloride) (PDADMAC) and Poly(sodium 4-styrenesulfonate) (PSS) are both strong polyelectrolytes and PE-NF membranes composed of PDADMAC/PSS have proven stable in both acidic and basic conditions (Elshof et al., 2020).

In this study, PDADMAC/PSS membranes are fabricated and evaluated for performance stability in hydroxide/carbonate and hydroxide/phosphate separations. The dependence of separation performance, particularly ion-ion selectivity, on the number of bilayers and solution conditions including pH, carbonate or phosphate concentrations, and carbonate/hydroxide or phosphate/hydroxide molar ratios, is examined. The performance stability of PDADMAC/PSS and commercial polyamide NF membranes (NF270) are compared to demonstrate how each membrane resists alkaline hydrolysis and changes in separation performance.

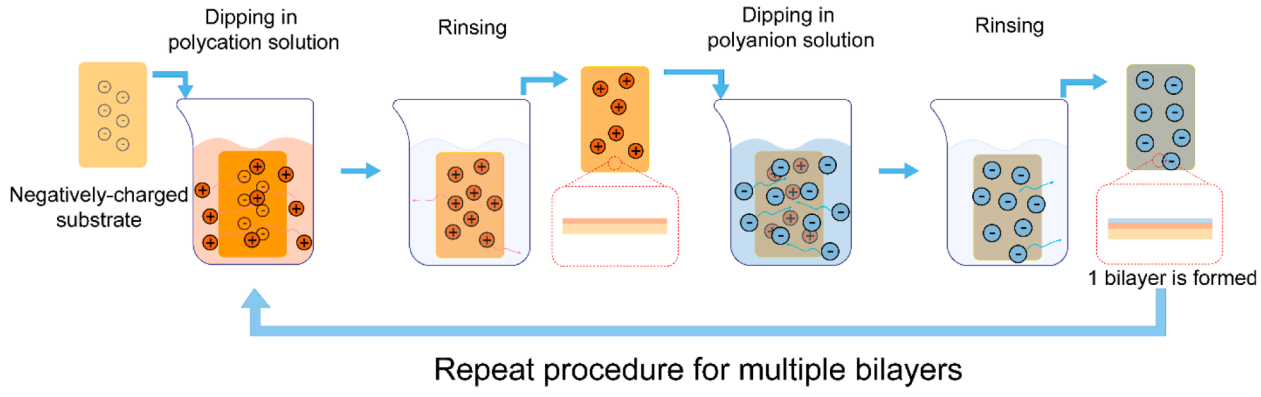

Fig. 1. Schematic representation of the LbL assembly process on a negatively charged PES substrate.

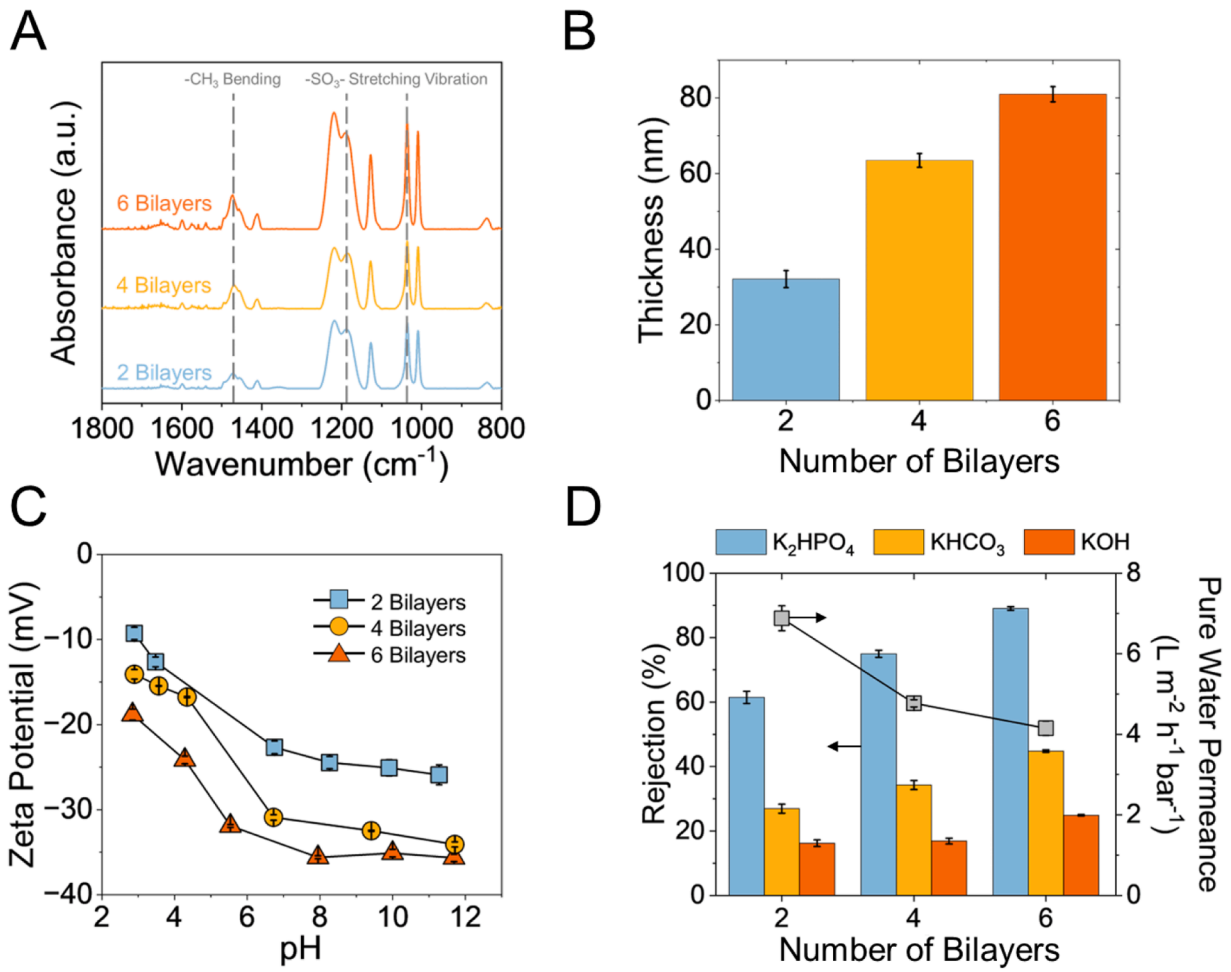

Fig. 2. (A) PM-IRRAS spectra of the 2, 4, and 6-bilayer PDADMAC-PSS films on a carboxylic acid-terminated gold surface, (B) thicknesses of 2,4, and 6-bilayer PDADMAC/PSS membranes on Si/COOH-terminated surfaces as determined by ellipsometry, (C) zeta potential as a function of deposited PDADMAC-PSS bilayers, and (D) single solute rejection (3 g L^{-1}) of relevant species (K2HPO4, KHCO3, and KOH). The feed solution pHs were 9.4 for K_2HPO_4, 8.3 for KHCO3, and 12.7 for KOH.

2. Materials and methods

2.1. Materials

Hydrophilic polyethersulfone (PES) ultrafiltration (UF) membranes manufactured by Microdyn Nadir with a molecular weight cutoff (MWCO) of 50 kDa were purchased from Sterlitech. PES UF supports are reportedly stable during long term exposure to pH 0–14 solutions. Polycation and polyanion solutions, PDADMAC (MW: 200–350 kDa, 20 wt % in H_2O) and PSS (MW: ~200 kDa, 30 wt% in H_2O), respectively, were both purchased from Sigma Aldrich, Inc. $MgSO_4$, KOH, $KHCO_3$, K_2CO_3, and K_2HPO_4 were all provided by Sigma Aldrich, Inc. Deionized water was used to prepare polyelectrolyte solutions and feed solutions. 11-Mercaptoundecanoic acid (95.0 %) was purchased from Sigma-Aldrich, Inc. and 10-undecenyltrichlorosilane (10-UTS, 97.0 %) was obtained from Gelest, Inc. Anhydrous toluene (99.8 %) was purchased from Sigma Aldrich, Inc. H_2O_2 (30.0 %), H_2SO_4 (> 95.0 %), HCl (36.5–38.0 % w/w), $KMnO_4$ (>99.0 %), and $NaIO_4$ (> 99.8 %) were purchased from Thermo Fisher Scientific, Inc. Single-side polished, boron-doped p-type silicon wafers ⟨100⟩ were purchased from University Wafer Inc. and Pure Wafer, respectively, with the latter used as a substrate for gold deposition. Chromium-coated tungsten rods were purchased from R.D. Mathis. Gold shot (99.9 %) was obtained from J&J Materials.

2.2. Polyelectrolyte membrane fabrication

PES UF supports were soaked in DI water at 20 °C for at least 12 h to remove any impurities and to completely wet their pores and surfaces. Pre-soaked PES UF supports were immersed in the polycation solution (1 g L^{-1} PDADMAC, 7 g L^{-1} $MgSO_4$) for 25 min, then immersed in a DI water solution for 5 min to remove any loosely bound polyelectrolytes from the membrane surface (Fig. 1). Then, the membranes were immersed in the polyanion solution (1.5 g L^{-1} PSS, 10 g L^{-1} $MgSO_4$) for 25 min and rinsed with DI water for 5 min to complete the fabrication of one PDADMAC/PSS bilayer. Rinsing solutions were regularly refreshed to prevent cross-contamination of the polyelectrolyte solutions. The LbL process was repeated until the desired number of bilayers was achieved. Upon completion, the membranes were dried under a fume hood at room temperature for at least 12 h before testing.

2.3. Preparation of carboxylic acid-terminated surfaces

Carboxylic acid-terminated gold and silicon substrates were fabricated as described in Sections S1.1 and S1.2 to mimic the negatively charged PES surface. The LbL process was performed on each surface under identical conditions as specified in Section 2.2. The substrates were used to fabricate PDADMAC/PSS membranes for Polarization Modulation Infrared Reflection Absorption Spectroscopy (PM-IRRAS) and ellipsometry, as these characterizations could not be directly

conducted on PES substrates.

2.4. Zeta potential measurements

Zeta potential measurements (SurPASS electrokinetic analyzer) were performed directly on PDADMAC/PSS membranes prepared on PES UF supports. Before beginning measurements, the pH of a 1 mM KCl solution was manually increased using a dilute solution prepared from KOH pellets (Sigma Aldrich). HCl (0.1 M) was added dropwise to the electrolyte solution to reduce the pH of the solution from alkaline to acidic throughout the duration of the experiment. The SurPASS measured the zeta potential four times at several points within the pH range of interest.

2.5. Membrane testing

The separation performance of PDADMAC/PSS membranes was tested using stainless steel crossflow filtration cells with an effective surface area (A) of 7.1 cm^2. The applied pressures were monitored by pressure gauges in each line. All membranes were compacted at 6 bar for 1 h before performing pure water permeance or rejection tests. Pure water permeance (L m^{-2} h^{-1} bar^{-1}) was calculated by measuring the volume of DI water that permeated through membrane (ΔV) over a certain time period (Δt) at an applied pressure (ΔP):

$$PWP = \frac{\Delta V}{A \Delta t \Delta P} \quad (1)$$

Single salt rejection (R) was determined by measuring the conductivity in the feed (C_F) and permeate (C_P) solutions:

$$R = \left(1 - \frac{C_P}{C_F}\right) \quad (2)$$

Each pure water permeance and solute rejection test was performed under the same conditions ($\Delta P = 6$ bar, $T = 20$ °C). Ion-ion selectivity ($S_{A/B}$) is the ratio of the feed concentration-normalized molar fluxes between the two species to be separated (A vs. B, or in our case, OH^- vs. CO_3^{2-} or PO_4^{3-}):

$$S_{A/B} \equiv \frac{J_A / C_{F,A}}{J_B / C_{F,B}} = \frac{1 - R_A}{1 - R_B} \quad (3)$$

where J_A (J_B), $C_{F,A}$ ($C_{F,B}$), and R_A (R_B) are the molar flux, molar concentration, and rejection for species A (B), respectively. Hydroxide rejections were determined by measuring the pH of the feed and permeate solutions and converting the pH to OH^- concentration. The carbonate and phosphate concentrations were determined by performing titrations using an automatic titrator (Fisher Scientific's Orion Star T910 pH Titrator). During the titration, a known volume of sample was carefully titrated from the initial pH to the endpoint using 1 M HCl as a titrant. Samples were tested immediately after filtration tests to prevent CO_2 dissolution into alkaline samples. Titration methods are commonly used to detect the concentration of carbonates and phosphates in mixtures. Generally, acid-base equilibrium and charge balance expressions can be utilized to quantify the molar concentration of carbonates or phosphates in samples (Figueira et al., 2023; Li et al., 2011; Morgante et al., 2024; Salvatore and Salvatore, 2014). A MATLAB-based program was used to analyze the titration curve from the automatic titrator and calculated the carbonate and phosphate concentrations. The equilibrium expressions and charge balance expressions used to analyze the titration curve are in the Supporting Information.

3. Results and discussion

3.1. Membrane properties and NF performance

The IR spectra reveal the successful incorporation of PDADMAC and PSS into each polyelectrolyte multilayer membrane, as evidenced by peaks at 1468 cm^{-1} (-CH_3 bending in PDADMAC), 1184 cm^{-1} (symmetric -SO_3- stretching vibrations), and 1040 cm^{-1} (asymmetric -SO_3- stretching vibrations) (Fig. 2A) (Eneh et al., 2020; Yang et al., 2002). The thickness of the COOH-terminated surface (1.6 nm) was subtracted from total thicknesses of the 2, 4, and 6-bilayer membranes to obtain PDADMAC/PSS multilayer thicknesses of 32.1 ± 2.2, 63.5 ± 1.8, and 81.0 ± 2.0 nm (Fig. 2B). Throughout the entire pH range, the 6-bilayer PE-NFM is the most negatively charged, while the 2-bilayer membrane is the least negatively charged. The increase in zeta potential as the electrolyte solution grows more acidic is commonly observed in PDADMAC/PSS membranes and is potentially attributed to H^+ adsorption to the negatively charged membrane surface (Cheng et al., 2018; Junker et al., 2023; Wang et al., 2021). Membranes for base recovery separations should be highly negatively charged to maximize the Donnan exclusion mechanism and minimize the impact of charge screening as the feed solution concentration increases. Between pH of 7 and 11.5, the zeta potential of 2, 4, and 6 bilayer membranes remains relatively constant, likely because PDADMAC and PSS are classified as 'strong' polyelectrolytes that are fully ionized under neutral and basic conditions (Fig. 2C). Thus, any appreciable changes in ion rejection as the pH of the feed solution increases should not be attributed to changes in membrane charge density.

Pure water permeance is the highest in 2-bilayer membranes (6.9 ± 0.3 L m^{-2} h^{-1} bar^{-1}) and lowest in 6-bilayer membranes (4.2 ± 0.2 L m^{-2} h^{-1} bar^{-1}) due to the increasing water transport resistance as membranes grow thicker (Fig. 2B and 2D). K_2HPO_4 and $KHCO_3$

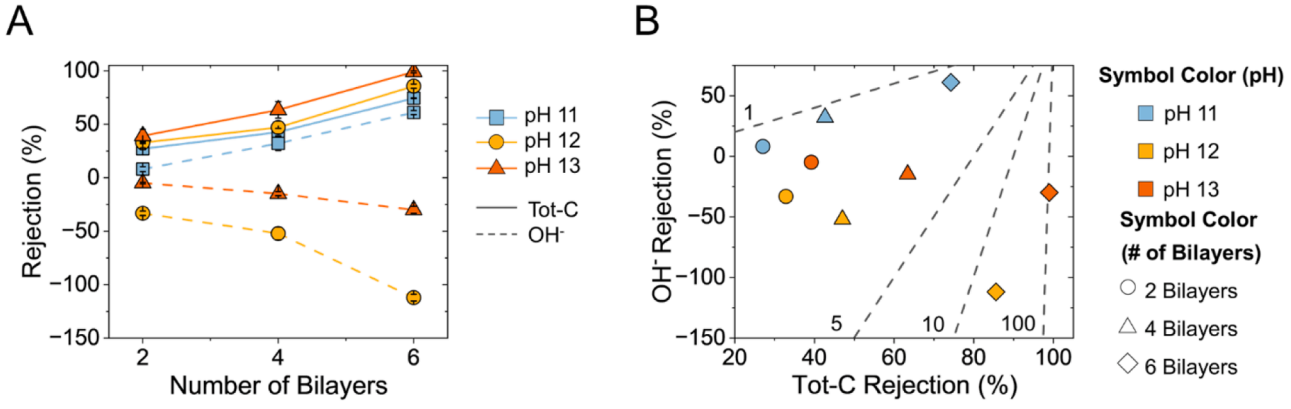

Fig. 3. (A) PDAMDAC/PSS membrane performance in OH^-/tot-C separations as the number of bilayers varies. The impact of the feed solution pH is investigated while the tot-C concentration remains fixed at 3 g tot-C L^{-1}. (B) $S_{OH^-/Tot-C}$ of PDADMAC/PSS membranes as the pH and number of bilayers varies. Tot-C concentrations remain constant at 3 g of tot-C L^{-1}. Dashed lines represent lines of constant $S_{OH^-/Tot-C}$.

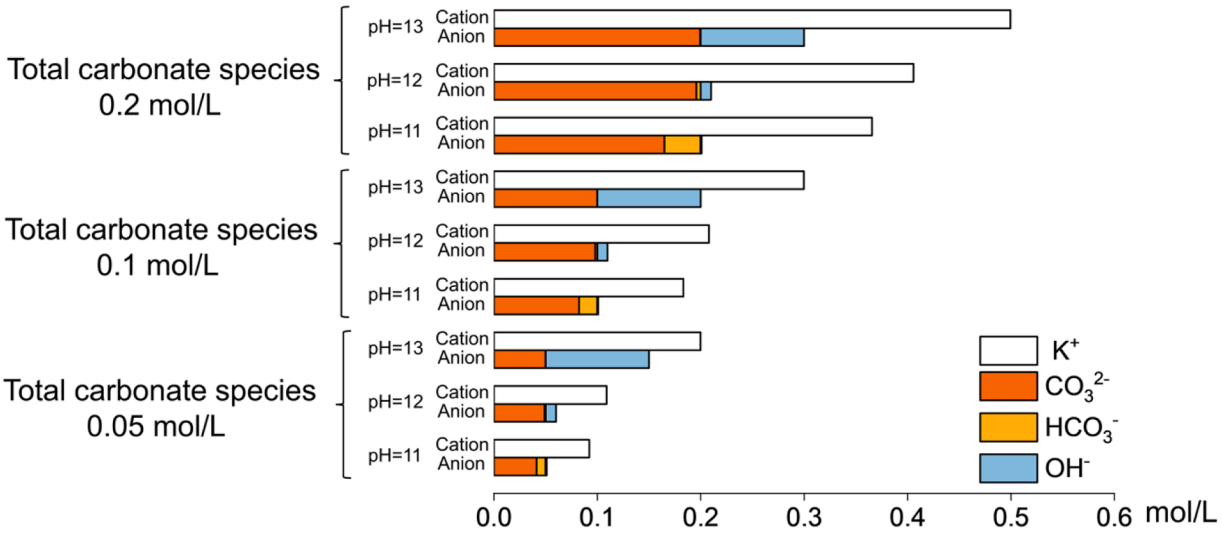

Fig. 4. NF feed solution compositions in molar equivalents of CO_3^{2-}, HCO_3^-, and OH^- with varying pH (11, 12, and 13) and tot-C concentrations (0.05, 0.1, and 0.15 M). The bar chart demonstrates how the distribution of anions shift with the feed solution conditions, providing insight into mixed salt separation performance.

rejections increase with the number of PDADMAC/PSS bilayers. K_2HPO_4 rejection increases from 61.4 % using the 2-bilayer membrane to 89.1 % using the 6-bilayer membrane (Fig. 2D). Similarly, $KHCO_3$ rejection increases from 26.9 % to 44.8 % (Fig. 2D). Less drastic increases in KOH rejection were observed as the number of bilayers increases, with the 2, 4, and 6-bilayer membranes achieving only 16.2 %, 16.9 %, and 24.9 % KOH rejection, respectively (Fig. 2B). Comparing the single salt rejections of $KHCO_3$ and K_2HPO_4 to KOH does not fully inform how mixed salt systems would perform under alkaline conditions; the 6-bilayer membrane rejects less than 50 % of $KHCO_3$ at pH 8.3 but its performance improves drastically as the pH of the feed solution increases.

The size and charge of phosphate and carbonate species vary significantly as the pH of the feed solution increases. Thus, the ion transport and separation performance are strongly dependent on phosphate and carbonate speciation. Since the net valence of carbonate and phosphate species increases with pH, a negatively charged membrane is expected to reject these anions more effectively as the pH increases. Carbonate and phosphate speciation is detailed in the Supporting Information (Fig. S1). As pH increases, steric exclusion is expected to be enhanced due to the increased hydrodynamic radii of ions with a higher valence; Donnan exclusion is stronger due to increased electrostatic repulsion of ions from the membrane surface, and dielectric exclusion increases due to increasing valence with pH. For simplicity, all carbonate species will be referred to as tot-C (total molarity of carbonate species) and all phosphate species will be referred to as tot-P (total molarity of phosphate species) throughout the rest of this paper. The molarity of carbonate and phosphate solutions (feed and permeate) are quantified using the titration method. Similarly, the $KOH/KHCO_3$ and KOH/K_2HPO_4 separations will be simply referred to as OH^-/tot-C and OH^-/tot-P separations.

3.2. Hydroxide/Carbonate separation

The number of PDADMAC/PSS bilayers has a marked impact on OH^-/tot-C separation performance. The 2-bilayer membrane is the least effective; the rejection of carbonate species only marginally increases with the pH and remains less than 40 % under all conditions (Fig. 3A). At pH 11, the 2-bilayer membrane rejects 27.1 ± 0.8 % of carbonate species and 8.1 ± 2.4 % of OH^-, yielding very low OH^-/tot-C selectivity (Fig. 3B, selectivity marked by the dashed lines). Increasing the feed solution's pH to 12 marginally increased carbonate rejection to 33.9 ± 0.9 % but resulted in a negative OH^-rejection of −33.2 ± 2.1 % (Fig. 3A).

Negative ion rejection is a widely reported phenomenon that often occurs when a highly excluded co-ion cohabitates the feed with a smaller, more mobile co-ion (Li et al., 2011; Xuerui et al., 2024). In our case, the small counter-ions (H^+ or K^+) are attracted to the negatively charged membrane and face minimal steric and dielectric exclusion resistance partitioning into the active layer. Co-ions must also travel through the membrane with the counter-ions to maintain electroneutrality in the membrane phase and permeating solution. When one co-ion species is highly excluded from the membrane (in our case CO_3^{2-}), the more permeable co-ion species preferentially pairs with the counter-ions. In other words, the need to maintain electroneutrality in the permeate increases the driving force for OH^- transport and accelerates its transport across the membrane.

Ion transport behavior is more complicated at pH 11 because the feed solution contains three co-ions that must be considered: CO_3^{2-}, HCO_3^-, and OH^- (Fig. 4). All three species are reactive and exist in equilibrium with one another. At lower pH, HCO_3^- is more abundant and is a source of proton as the pH increases. At pH 11, 12.5 % of carbonate species exist in the HCO_3^- form with the remaining 87.5 % in the CO_3^{2-} form (**Fig. S1A, S1C**, and **4**). Both PDADMAC/PSS and commercial NF270 membranes can discriminate between carbonate species and exhibit positive OH^- rejection at pH 11. HCO_3^- is more mobile than CO_3^{2-}, and its selective transport lowers the CO_3^{2-}/HCO_3^- molar ratio inside the membrane pores relative to the feed solution. As a result, the reactive HCO_3^- is driven to re-establish equilibrium in its new environment. Models describing water and ion transport through NF and RO membranes predict that acid-base equilibrium reactions are very rapid compared to ion transport, allowing such reactions to take place within the confined environment of the pore (Biesheuvel et al., 2020; Dykstra et al., 2014). The HCO_3^- species donate protons to OH^-, forming H_2O and thereby reducing the pH of the permeate stream. Experimental results in similar systems have also observed sizable reductions in the permeate pH when both HCO_3^- and CO_3^{2-} are present and attribute the lower permeate pH to the re-establishment of carbonate equilibrium within the pores (Padilla and Saitua, 2010; Zhu et al., 2007). However, the interplay between HCO_3^-/CO_3^{2-} species selectivity and reactive transport is less pronounced when a membrane rejects both HCO_3^- and CO_3^{2-} very well. For example, the commercial NF90 membrane rejects >99 % of all carbonate species at pH 11 and exhibits negative OH^- rejection (**Fig. S3**). In this case, OH^- is the only anion capable of maintaining electroneutrality in the permeate, ultimately accelerating OH^- transport across the membrane and increasing the pH of the permeate solution relative to the feed solution (**Fig. S3**).

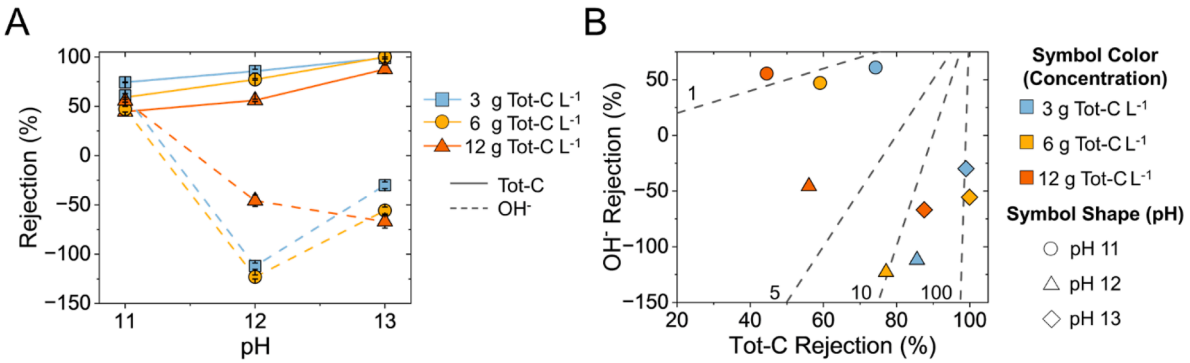

Fig. 5. (A) The performance of the 6-bilayer PDADMAC/PSS membrane in OH^-/tot-C separations as the pH (11, 12, and 13) and tot-C concentration (3, 6, and 12 g PO_4^{3-} L^{-1}) in the feed solution vary. (B) The impact the feed solution pH and tot-C concentration have on $S_{OH^-/tot-C}$ is investigated. Dashed lines represent lines of constant $S_{OH^-/tot-C}$.

At pH 12, nearly all carbonate species are in the divalent anion form, minimizing HCO_3^- driven reactive transport (Fig. 4). As such, negative OH^- rejection is observed at pH 12 for the 2-bilayer membrane (Fig. 3A). At pH 13, the carbonate rejection of the 2-bilayer membrane increases to 39.2 ± 6.0 % while OH^- rejection is −4.9 ± 0.7 % (Fig. 3A). The tot-C rejection continues to increase with the pH because carbonate species face increasingly greater Donnan exclusion from the membrane as they deprotonate into the divalent anion form (**Fig. S1A** and **S1C**). However, the OH^- rejection is less negative at pH 13 than it is at pH 12. The counter-ions (K^+) provided by highly excluded co-ions (CO_3^{2-}) are responsible for promoting the transport of lesser excluded co-ions (OH^-) through the membrane. When CO_3^{2-} is present at much greater concentration than OH^-, the counter-ions provided by CO_3^{2-} are abundant and their transport in turn drives the trans-membrane transport of a significant portion of OH^- to the permeate, thus leading to negative rejection. However, increasing the pH by a unit decreases the tot-C/OH^- molar ratio by a factor of 10. The tenfold increase in OH^- concentration reduces the driving force (i.e., K^+/OH^- molar ratio, Fig. 4) and thus reduces the proportion of OH^- from the feed solution required to travel across the membrane with K^+ to maintain electroneutrality.

The 2-bilayer membrane is loose and incapable of precise separations, so the magnitude of negative rejection and $S_{OH^-/tot-C}$ are low under all conditions investigated (Fig. 3B). The 4-bilayer membrane performs better than the 2-bilayer membrane, but tot-C rejection approaches only 63.4 ± 7.7 % at pH 13 while $S_{OH^-/tot-C}$ remains below 5 (Fig. 3A and 3B). The OH^-/tot-C separation is much more effective using the 6-bilayer PDADMAC/PSS membrane. The 6-bilayer performs better than the 2 and 4-bilayer membranes, exhibiting tot-C rejections > 99 % at pH 13 and >85 % at pH 12. Higher tot-C rejection in 6-bilayer membranes is attributable to the increased Donnan (electrostatic) exclusion of carbonate from a more negatively charged membrane surface (Fig. 2C) and the enhanced steric exclusion of ions from membranes with smaller pores. The rejection of OH^- is the most negative for the 6-bilayer membrane due to enhanced ability of the membrane to reject CO_3^{2-} (Fig. 3A). Therefore, $S_{OH^-/tot-C}$ exceeds 10 at pH 12 and exceeds 100 at pH 13. The OH^-/tot-C separation was the most selective at pH 13 where the 6-bilayer PDADMAC/PSS membrane rejected virtually all the tot-C species. In the context of carbon capture, the pH of KOH capture solvents typically exceeds 12 (Bandi et al., 1995; Keith et al., 2018; Rouxhet et al., 2022).

The impact the tot-C/OH^- molar ratio has on separation performance is investigated using the best-performing 6-bilayer membrane (Fig.5). Tot-C rejection increased with the pH but decreased with increasing tot-C concentration in the feed solution. Charge screening is more severe as salt concentration increases, limiting the role Donnan mechanism plays in excluding co-ions (Fig. 5A). Consequently, the tot-C concentration and feed solution pH also influence OH^- rejection. For each tot-C concentration investigated, OH^- rejection decreased from positive to negative when the pH was increased from 11 to 12 (Fig. 5A). A minimum OH^- rejection was observed at pH 12 for the lower concentrations (3 and 6 g of tot-C L^{-1}), but behavior deviated from this trend when the feed solution concentration was 12 g tot-C L^{-1}.

At the highest tot-C concentration, OH^- rejection was less negative at pH 12 than it was for the lower tot-C concentrations. The tot-C rejection increased to nearly 90 % when the pH of the feed solution was 13 (Fig. 5A). High tot-C rejection, along with the presence of more permeable counter-ions (i.e., K^+) at the highest tot-C concentration, enhanced the driving force for accelerated OH^- transport through the membrane relative to the lower concentrations. As such, OH^- rejection was more negative than it was at pH 12 (Fig. 5A). Overall, the $S_{OH^-/tot-C}$

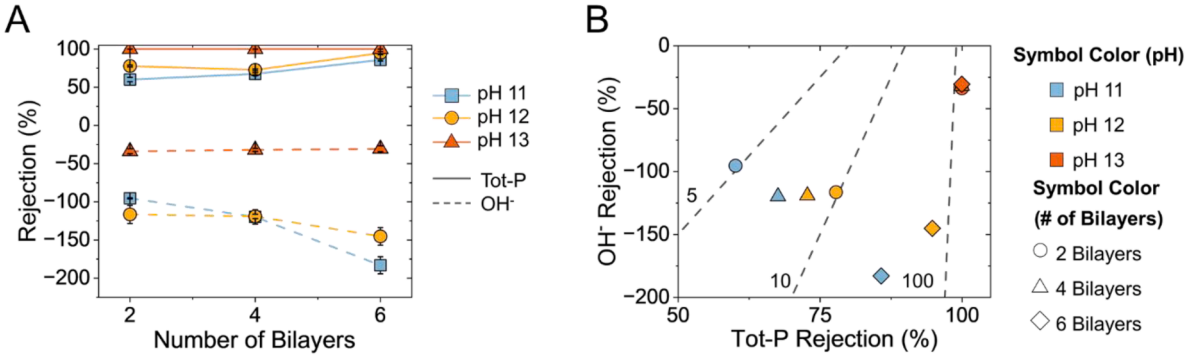

Fig. 6. (A) PDADMAC/PSS membrane performance in OH^-/tot-P separations as the number of bilayers varies. The impact of the feed solution pH is investigated while the tot-P concentration remains fixed at 3 g tot-P L^{-1}. (B) $S_{OH^-/PO_4^{3-}}$ of PDADMAC/PSS membranes as the pH and number of bilayers varies. tot-P concentrations in the feed solution remain constant at 3 g of tot-P L^{-1}. Dashed lines represent lines of constant $S_{OH^-/PO_4^{3-}}$.

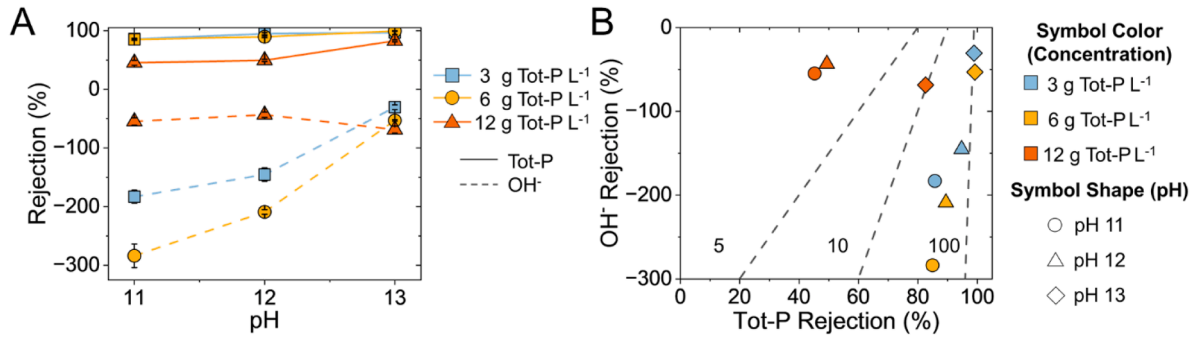

Fig. 7. (A) The performance of the 6-bilayer PDADMAC/PSS membrane in OH^-/tot-P separations as the pH (11, 12, and 13) and tot-P concentration (3, 6, and 12 g tot-P L^{-1}) in the feed solution varies. (B) The impact the feed solution pH and tot-P concentration has on $S_{OH^-/Tot-P}$ is investigated. Dashed lines represent lines of constant $S_{OH^-/Tot-P}$.

for 3 and 6 g tot-C L^{-1} are comparable due to similar trends in tot-C and OH^- rejection (Fig. 5B). The $S_{OH^-/tot-C}$ decreased with lower pH and was around 1 at pH 11 due to similar rates of OH^- and tot-C rejection (Fig. 5B). With the same pH, the $S_{OH^-/tot-C}$ was the lowest at the highest tot-C concentration (Fig. 5B) because of the reduced rejection of tot-C and the generally less negative OH^- rejection at lower tot-C concentration (except for 12 g tot-C L^{-1} at pH 13).

3.3. Hydroxide/Phosphate separation

The same principle governing OH^-/tot-C separation applies to the OH^-/tot-P separation. Specifically, multivalent anion rejection generally increases with the pH and the number of PDADMAC/PSS bilayers. Since the net valence of phosphate species is higher than the net valence of carbonate species from pH 11–13, which results in a higher charge and larger hydrated radius for phosphate species, the OH^-/tot-P separation is generally more effective than the OH^-/tot-C separation. At pH 11, 98 % of phosphate species exist in the HPO_4^{2-} form (**Fig. S1B, S1D**, and **S2**). Thus, negative OH^- rejection is observed for each membrane. The OH^- rejection at pH 11 is approximately −100 % with both the 2 and 4-bilayer membranes and −183.2 ± 11.2 % with the 6-bilayer membrane (Fig. 6A). Phosphate species rejection increases from 60.1 ± 2.8 % ($S_{OH^-/tot-P} \sim 5$) with the 2-bilayer membrane to 85.8 ± 1.6 % ($S_{OH^-/tot-P} \sim 20$) with the 6-bilayer membrane, making separation at pH 11 fairly effective (Fig. 6A and 6B).

The 6-bilayer membrane is even more effective at a higher pH due to the increased valence of phosphate species. The 6-bilayer PDADMAC/PSS membranes remove ~95 % of tot-P at pH 12 ($S_{OH^-/tot-P} > 45$) and nearly all tot-P at pH 13 ($S_{OH^-/tot-P} > 100$) (Fig. 6A and 6B). In fact, the 2, 4, and 6-bilayer membranes are equally capable of separating OH^- from phosphates (82 % in the form of PO_4^{3-}) at pH 13 due to the significant difference between the two species in the extent of Donnan, dielectric, and steric exclusion (**Fig. S1B** and **S1D**).

The 6-bilayer membrane performs similarly for low tot-P concentrations (3 and 6 g tot-P L^{-1}) (Fig. 7A and 7B). The separation is very effective under these conditions ($S_{OH^-/tot-P} > 20$) and produces high-purity OH^- streams at pH 13 (Fig. 7B). Since tot-P rejections are similar for 3 and 6 g tot-P L^{-1}, the extent of negative OH^- rejection is greater when the tot-P concentration is 6 g tot-P L^{-1} (Fig. 7A). The multivalent-monovalent anion molar ratio in the feed solution again proves critical in establishing the driving force for accelerated OH^- transport across the membrane. Charge screening at 12 g tot-P L^{-1} lowers tot-P rejection, limiting the extent of negative OH^- rejection and magnitude of $S_{OH^-/tot-P}$ (Fig. 7B). However, the tot-P concentration would begin with a small fraction of 12 g L^{-1} in practical applications, (Bacelo et al., 2020) thus a high tot-P concentration is only relevant toward the end of the module when the tot-P is concentrated to a great extent.

3.4. Alkaline stability of the PDADMAC/PSS membranes

The fabricated PDADMAC/PSS membranes retained their ability to perform base recovery separations for at least 28 days, while the polyamide NF270 membrane performance began to decline after 3 days of exposure to pH 13 KOH solutions (Fig. 8A and 8B). The pH of the storage solution has minimal impact on the stability of strong polyelectrolyte pairings, as both PDADMAC and PSS remain fully ionized at pH 13. Instead, the solution molarity poses a greater threat to the structural integrity of PE-NF membrane selective layers (Han et al., 2012). PDADMAC/PSS membranes are shown to experience significant mass loss when the molarity of a storage solution exceeds 2 M, though this threshold may vary depending on the nature of the salt used (Digby et al., 2022; Han et al., 2012; Klitzing et al., 2004). In this case, the relatively low ionic strength (0.1 M) is insufficient for competing ions to

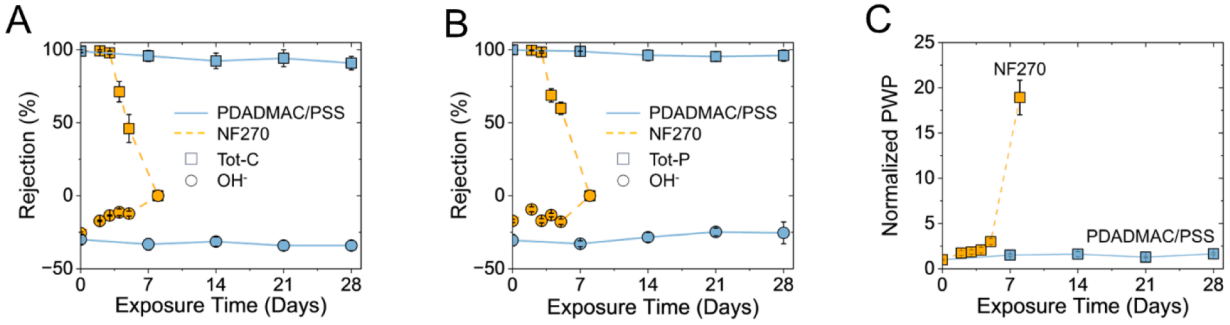

Fig. 8. The performance of PDADMAC/PSS and NF270 membranes during long-term exposure to pH 13 KOH is gauged by (A) 3 g tot-C L^{-1} separation performance at pH 13 and (B) 3 g tot-P L^{-1} at pH 13. The pure water permeance of (C) PDADMAC/PSS and NF270 membranes. Each data point represents a different membrane sample. The pressure was maintained at 6 bar for each filtration test.

Table 1
Summary of the salt rejection, water permeance, and alkaline solution exposure conditions for various alkaline-resistant nanofiltration membranes.

Membrane Composition	Permeance Before (L m^{-2} h^{-1} bar^{-1})	Permeance After (L m^{-2} h^{-1} bar^{-1})	Salt Rejection Before (%)	Salt Rejection After (%)	Exposure Conditions	Ref
PVA-APES-1.0	0.67	0.69	98.5[a]	97.1[a]	4 % w/v NaOH (30 d)	(Zhang et al., 2014)
PEI-0.3/PP-0.2/PDI-0.2	0.65	1.3	99.0[b]	94.6[b]	20 % w/v NaOH (390 d)	(Zhang et al., 2022)
PEI/CC-PDI	1.3	2.7	99.1 %[b]	96.0 %[b]	20 wt% NaOH (150 d)	(Zhao et al., 2023)
MPD-tBrMeB	1.2	1.7	67.3 %[b]	69.9 %[b]	0.1 M NaOH (33 d)	(Asadi Tashvigh et al., 2021)
PVA-SMPTES	2.2	2.9	96 %[a]	95.3 %[a]	0.1 M NaOH (30 d)	(Zhang et al., 2015)
PDADMAC/PSS	12.5	10.6	95.5[b]	96.1[b]	0.1 M NaOH (66 d)	(Elshof et al., 2020)
PEI-0.4/PDI-0.25	2.5	2.6	97.6[b]	91.8[b]	20 % w/v NaOH (365 d)	(Zhang et al., 2021)
PES-g-PAA	1.5	3.6	95.6[a]	85.9[a]	2 M NaOH (30 d)	(Guo et al., 2024)
PES-g-PDMAPS	2.4	3.4	88.4[a]	77.8[a]	2 M NaOH	(Guo et al., 2024)
PDADMAC/PSS	4.2	6.8	99.2 %[c] 99.5 %[d]	90.9 %[c] 96.1 %[d]	0.1 M KOH (28 days)	This Work

Notes: a refers to Na_2SO_4 rejection, b refers to $MgSO_4$ rejection, c refers to tot-C rejection when the feed solution pH is 13, and d refers to tot-P rejection when the feed solution pH is 13.

disrupt the polyelectrolyte pairings and compromise the active layer.

By day 8, rejections of all ions by the NF270 membrane approached 0. The poor stability of the NF270 membrane is attributable to the irreversible amide bond hydrolysis which de-crosslinks the polyamide active layer and renders these membranes unsuitable for base recovery applications. Fluctuations in tot-C and tot-P rejections over the weeks were attributed to natural variations in our PDADMAC/PSS membrane samples prepared for the study (Fig. 8A and 8B).

Each week, three fresh membrane samples were removed from the pH 13 KOH solution for testing (Fig. 8A and 8B). The PWP of the 6-bilayer PDADMAC/PSS membrane increased beyond 6 L m^{-2} h^{-1} bar^{-1} after one week of exposure to pH 13 KOH solution but stabilized near this value for the entire exposure test of 28 days (Fig. 8C). The increase and subsequent stabilization in water permeance is attributed to the wetting, relaxation, and rearrangement of polyelectrolyte chains in water. In contrast, the control membrane (day 0) was stored dry after fabrication and tested without exposure to aqueous conditions. The NF270 membrane active layer undergoes significant changes throughout the exposure test. By day 8, PWP increases from 14.7 ± 0.7 to nearly 300 L m^{-2} h^{-1} bar^{-1} (i.e., over 20 times of the initial flux), which suggests the polyamide active layer has been fully destroyed (Fig. 8C).

Table 1 details the performance and stability of NF membranes designed to retain multivalent anions. Several membranes demonstrate exceptional resistance to alkaline hydrolysis and maintain impressive salt rejections during exposure to alkaline conditions. Notably, polyelectrolyte membranes combine stability with moderate to high permeances, showcasing their potential for efficient base separations. The PDADMAC/PSS membranes developed for this study maintained outstanding performance in the OH^-/tot-C and OH^-/tot-P separations, underscoring their suitability as robust, high-performance candidates for alkaline separations processes.

4. Conclusion

In this study, we investigated the fabrication and performance of PE-NF membranes for base recovery and concentration of the multivalent anions (phosphate and carbonate) in the context of nutrient recovery and carbon capture. Below are the key observations from both separations of carbonate and phosphate from hydroxide ions:

(1) Increasing the pH of the feed solution improves selectivity due to the impact carbonate or phosphate speciation has on ion partitioning and transport.
(2) The selectivity is higher at low-to-moderate concentrations of phosphate or carbonate because a very high phosphate or carbonate concentration undermines the Donnan exclusion and the rejection of the multivalent anions.
(3) PDADMAC/PSS membranes have superior stability (in terms of water flux and ion rejections) as compared to commercial polyamide membrane (NF270) under long-term exposure to alkaline conditions.

The fabricated PDADMAC/PSS membranes were capable of retaining > 90 % of tot-C and tot-P species while achieving negative rejection of OH^- for up to four weeks at pH 13. Overall, our work demonstrates the potential of using polyelectrolyte-based alkaline-resistant NF membranes for recovering base and concentrating multivalent anions in sustainability applications.

CRediT authorship contribution statement

Joshua L. Livingston: Writing – original draft, Visualization, Methodology, Investigation, Formal analysis, Data curation, Conceptualization. **Abigail Cafferty:** Methodology, Investigation. **Riley Miller:** Investigation, Data curation. **Allison V. Cordova-Huaman:** Investigation, Data curation. **Jin Zhang:** Visualization, Investigation, Formal analysis. **G. Kane Jennings:** Writing – review & editing, Supervision, Project administration, Investigation, Funding acquisition, Formal analysis. **Shihong Lin:** Writing – review & editing, Project administration, Investigation, Funding acquisition, Conceptualization.

Declaration of competing interest

The authors declare no financial interest or COI for the manuscript submitted.

Acknowledgement

This work is funded partially by the US-Israel Binational Agricultural Research and Development Fund (BARD; grant No. IS-5209–19) and partially by the US-Department of Energy (DE-FE 0032125).

Supplementary materials

Supplementary material associated with this article can be found, in the online version, at doi:10.1016/j.watres.2025.123127.

Data availability

Data will be made available on request.

References

Arkell, A., Krawczyk, H., Thuvander, J., Jönsson, A.S., 2013. Evaluation of membrane performance and cost estimates during recovery of sodium hydroxide in a hemicellulose extraction process by nanofiltration. Sep. Purif. Technol. 118, 387–393. https://doi.org/10.1016/j.seppur.2013.07.015.

Asadi Tashvigh, A., Elshof, M.G., Benes, N.E., 2021. Development of thin-film composite membranes for nanofiltration at extreme pH. ACS Appl. Polymer Mater. J. 3, 5912–5919. https://doi.org/10.1021/acsapm.1c01172.

Bacelo, H., Pintor, A.M.A., Santos, S.C.R., Boaventura, R.A.R., Botelho, C.M.S., 2020. Performance and prospects of different adsorbents for phosphorus uptake and recovery from water. Chemic. Eng. J. 381, 122566. https://doi.org/10.1016/j.cej.2019.122566.

Bai, J., Lai, W., Gong, L., Xiao, L., Wang, G., Shan, L., Luo, S., 2022. Ionic liquid regulated interfacial polymerization process to improve acid-resistant nanofiltration membrane permeance. J. Memb. Sci. 641, 119882. https://doi.org/10.1016/j.memsci.2021.119882.

Bandi, A., Specht, M., Weimer, T., Schaber, K., 1995. CO_2 recycling for hydrogen storage and transportation —Electrochemical CO_2 removal and fixation. Energy Convers. Manage 36, 899–902. https://doi.org/10.1016/0196-8904(95)00148-7.

Biesheuvel, P.M., Zhang, L., Gasquet, P., Blankert, B., Elimelech, M., Van Der Meer, W.G. J., 2020. Ion selectivity in brackish water desalination by reverse osmosis: theory, measurements, and implications. Environ. Sci. Technol. Lett. 7, 42–47. https://doi.org/10.1021/acs.estlett.9b00686.

Cheng, W., Liu, C., Tong, T., Epsztein, R., Sun, M., Verduzco, R., Ma, J., Elimelech, M., 2018. Selective removal of divalent cations by polyelectrolyte multilayer nanofiltration membrane: role of polyelectrolyte charge, ion size, and ionic strength. J. Memb. Sci. 559, 98–106. https://doi.org/10.1016/j.memsci.2018.04.052.

Conley, D.J., Paerl, H.W., Howarth, R.W., Boesch, D.F., Seitzinger, S.P., Havens, K.E., Lancelot, C., Likens, G.E., 2009. Controlling eutrophication: nitrogen and phosphorus. Science 323, 1014–1015. https://doi.org/10.1126/science.1167755.

Cooper, J., Lombardi, R., Boardman, D., Carliell-Marquet, C., 2011. The future distribution and production of global phosphate rock reserves. Res., Conserv. Recycl. 57, 78–86. https://doi.org/10.1016/j.resconrec.2011.09.009.

Digby, Z.A., Yang, M., Lteif, S., Schlenoff, J.B., 2022. Salt resistance as a measure of the strength of polyelectrolyte complexation. Macromolecules. 55, 978–988. https://doi.org/10.1021/acs.macromol.1c02151.

Dykstra, J.E., Biesheuvel, P.M., Bruning, H., Ter Heijne, A., 2014. Theory of ion transport with fast acid-base equilibrations in bioelectrochemical systems. Physic. Rev. E 90, 013302. https://doi.org/10.1103/PhysRevE.90.013302.

Elshof, M.G., De Vos, W.M., De Grooth, J., Benes, N.E., 2020. On the long-term pH stability of polyelectrolyte multilayer nanofiltration membranes. J Memb Sci 615, 118532. https://doi.org/10.1016/j.memsci.2020.118532.

Eneh, C.I., Bolen, M.J., Suarez-Martinez, P.C., Bachmann, A.L., Zimudzi, T.J., Hickner, M.A., Batys, P., Sammalkorpi, M., Lutkenhaus, J.L., 2020. Fourier transform infrared spectroscopy investigation of water microenvironments in polyelectrolyte multilayers at varying temperatures. Soft. Matter. 16, 2291–2300. https://doi.org/10.1039/C9SM02478F.

Ferreira, D.A., Prados, L.M.Z., Majuste, D., Mansur, M.B., 2009. Hydrometallurgical separation of aluminium, cobalt, copper and lithium from spent Li-ion batteries. J. Power. Sources. 187, 238–246. https://doi.org/10.1016/j.jpowsour.2008.10.077.

Figueira, M., Rodríguez-Jiménez, D., López, J., Reig, M., Luis Cortina, J., Valderrama, C., 2023. Evaluation of the nanofiltration of brines from seawater desalination plants as pre-treatment in a multimineral brine extraction process. Sep. Purif. Technol. 322, 124232. https://doi.org/10.1016/j.seppur.2023.124232.

Geissler, B., Hermann, L., Mew, M.C., Steiner, G., 2018. Striving toward a circular economy for phosphorus: the role of phosphate rock mining. Minerals 8, 395. https://doi.org/10.3390/min8090395.

Gésan-Guiziou, G., Alvarez, N., Jacob, D., Daufin, G., 2007. Cleaning-in-place coupled with membrane regeneration for re-using caustic soda solutions. Sep. Purif. Technol. 54, 329–339. https://doi.org/10.1016/j.seppur.2006.10.007.

Guo, L., Yang, Y., Dong, D., Liang, F., Zhang, Y., Zhu, Y., Jin, J., Hou, L., 2024. Hydrophilic carbon-carbon covalent linkage network structure for strong acid/alkali resistant and antifouling nanofiltration membrane. J. Memb. Sci 693, 122356. https://doi.org/10.1016/j.memsci.2023.122356.

Han, L., Mao, Z., Wuliyasu, H., Wu, J., Gong, X., Yang, Y., Gao, C., 2012. Modulating the structure and properties of poly(sodium 4-styrenesulfonate)/poly(diallyldimethylammonium chloride) multilayers with concentrated salt solutions. Langmuir. 28, 193–199. https://doi.org/10.1021/la2040533.

Huang, J., Luo, J., Chen, X., Feng, S., Wan, Y., 2020. How do chemical cleaning agents act on polyamide nanofiltration membrane and fouling layer? Ind. Eng. Chem. Res. 59, 17653–17670. https://doi.org/10.1021/acs.iecr.0c03365.

Joshi, B., Prasetyo, E., Bandyopadhyay, S., 2024. Selective lithium recovery from pyrolyzed black mass through optimized caustic leaching. J. Environ. Chem. Eng. 12, 113787. https://doi.org/10.1016/j.jece.2024.113787.

Junker, M.A., Regenspurg, J.A., Valdes Rivera, C.I., Brinke, E.T., De Vos, W.M., 2023. Effects of feed solution pH on polyelectrolyte multilayer nanofiltration membranes. ACS. Appl. Polym. Mater. 5, 355–369. https://doi.org/10.1021/acsapm.2c01542.

Just, G., Pokorny, I., Pritzkow, W., 1995. Kinetic studies on the reaction of cyanuric chloride with amines. J. für praktische Chemie 337, 133–135. https://doi.org/10.1002/prac.19953370128.

Kar, S., Goeppert, A., Galvan, V., Chowdhury, R., Olah, J., Prakash, G.K.S., 2018. A carbon-neutral CO_2 capture, conversion, and utilization cycle with low-temperature regeneration of sodium hydroxide. J. Am. Chem. Soc. 140, 16873–16876. https://doi.org/10.1021/jacs.8b09325.

Keith, D.W., Holmes, G., St. Angelo, D., Heidel, K., 2018. A Process for Capturing CO_2 from the Atmosphere. Joule 2, 1573–1594. https://doi.org/10.1016/j.joule.2018.05.006.

Klitzing, R.V., Wong, J.E., Jaeger, W., Steitz, R., 2004. Short range interactions in polyelectrolyte multilayers. Curr. Opin. Colloid. Interface Sci. 9, 158–162. https://doi.org/10.1016/j.cocis.2004.05.022.

Labban, O., Liu, C., Chong, T.H., Lienhard V, J.H., 2017. Fundamentals of low-pressure nanofiltration: membrane characterization, modeling, and understanding the multi-ionic interactions in water softening. J. Memb. Sci. 521, 18–32. https://doi.org/10.1016/j.memsci.2016.08.062.

Lee, K.P., Bargeman, G., De Rooij, R., Kemperman, A.J.B., Benes, N.E., 2017. Interfacial polymerization of cyanuric chloride and monomeric amines: pH resistant thin film composite polyamine nanofiltration membranes. J. Memb. Sci 523, 487–496. https://doi.org/10.1016/j.memsci.2016.10.012.

Lee, K.P., Zheng, J., Bargeman, G., Kemperman, A.J.B., Benes, N.E., 2015. pH stable thin film composite polyamine nanofiltration membranes by interfacial polymerisation. J. Memb. Sci 478, 75–84. https://doi.org/10.1016/j.memsci.2014.12.045.

Li, L., Zhu, G., Tong, Y., Ding, K., Wang, Z., Meng, C., Gao, C., 2023. Polyethyleneimine modified polyamide composite nanofiltration membrane for separation of lithium and magnesium. J. Water. Process. Eng. 54, 103894. https://doi.org/10.1016/j.jwpe.2023.103894.

Li, X., Remias, J.E., Neathery, J.K., Liu, K., 2011. NF/RO faujasite zeolite membrane-ammonia absorption solvent hybrid system for potential post-combustion CO_2 capture application. J Memb Sci 366, 220–228. https://doi.org/10.1016/j.memsci.2010.10.007.

Ma, Q., Shuler, P.J., Aften, C.W., Tang, Y., 2015. Theoretical studies of hydrolysis and stability of polyacrylamide polymers. Polym. Degrad. Stab. 121, 69–77. https://doi.org/10.1016/j.polymdegradstab.2015.08.012.

Merin, U., Gésan-Guiziou, G., Boyaval, E., Daufin, G., 2002. Cleaning-in-place in the dairy industry: criteria for reuse of caustic (NaOH) solutions. Lait. 82, 357–366. https://doi.org/10.1051/lait:2002016.

Morgante, C., Lopez, J., Cortina, J.L., Tamburini, A., 2024. New generation of commercial nanofiltration membranes for seawater/brine mining: experimental evaluation and modelling of membrane selectivity for major and trace elements. Sep. Purif. Technol. 340, 126758. https://doi.org/10.1016/j.seppur.2024.126758.

Padilla, A.P., Saitua, H., 2010. Performance of simultaneous arsenic, fluoride and alkalinity (bicarbonate) rejection by pilot-scale nanofiltration. Desalination. 257, 16–21. https://doi.org/10.1016/j.desal.2010.03.022.

Paul, M., Jons, S.D., 2016. Chemistry and fabrication of polymeric nanofiltration membranes: a review. Polymer. 103, 417–456. https://doi.org/10.1016/j.polymer.2016.07.085.

Rouxhet, A., Kim, S., Leonard, G., 2022. Study of direct air capture (DAC) using a KOH/K_2CO_3 absorbing solution for CO_2 capture. SSRN J. https://doi.org/10.2139/ssrn.4273837.

Salvatore, M.M., Salvatore, F., 2014. Analysis of phosphate salts mixtures by a simple visual alkalimetric titration. J. Lab. Chem. Educ.

Sena, M., Seib, M., Noguera, D.R., Hicks, A., 2021. Environmental impacts of phosphorus recovery through struvite precipitation in wastewater treatment. J. Clean. Prod. 280, 124222. https://doi.org/10.1016/j.jclepro.2020.124222.

Song, Y., Li, T., Zhou, J., Li, Z., Gao, C., 2016. Analysis of nanofiltration membrane performance during softening process of simulated brackish groundwater. Desalination. 399, 159–164. https://doi.org/10.1016/j.desal.2016.09.004.

Su, Y., Peng, H., Liu, X., Li, J., Zhao, Q., 2024. High performance, pH-resistant membranes for efficient lithium recovery from spent batteries. Nat. Commun. 15, 10295. https://doi.org/10.1038/s41467-024-54503-8.

Thurston, J.T., Dudley, J.R., Kaiser, D.W., Hechenbleikner, I., Schaefer, F.C., Holm-Hansen, D., 1951. Cyanuric chloride derivatives. I. Aminochloro-s-triazines. J. Am. Chem. Soc. 73, 2981–2983. https://doi.org/10.1021/ja01151a001.

Wang, R., Alghanayem, R., Lin, S., 2023. Multipass nanofiltration for lithium separation with high selectivity and recovery. Environ. Sci. Technol. 57, 14464–14471. https://doi.org/10.1021/acs.est.3c04220.

Wang, Y., Zucker, I., Boo, C., Elimelech, M., 2021. Removal of emerging wastewater organic contaminants by polyelectrolyte multilayer nanofiltration membranes with tailored selectivity. ACS. ES. T. Eng. 1, 404–414. https://doi.org/10.1021/acsestengg.0c00160.

Xuerui, G., Ping, L., Yuan, Q., Chengling, B., Zhengyang, G., Shuili, Y., 2024. Negative rejection phenomenon in the mixed salt nanofiltration: law and mechanism. Desalination. 583, 117667. https://doi.org/10.1016/j.desal.2024.117667.

Yang, J.C., Jablonsky, M.J., Mays, J.W., 2002. NMR and FT-IR studies of sulfonated styrene-based homopolymers and copolymers. Polymer. 43, 5125–5132. https://doi.org/10.1016/S0032-3861(02)00390-7.

Yang, Z., Long, L., Wu, C., Tang, C.Y., 2022. High permeance or high selectivity? Optimization of system-scale nanofiltration performance constrained by the upper bound. ACS. ES. T. Eng. 2, 377–390. https://doi.org/10.1021/acsestengg.1c00237.

Yu, L., Zhang, Y., Xu, L., Liu, Q., Borjigin, B., Hou, D., Xiang, J., Wang, J., 2020. One step prepared Janus acid-resistant nanofiltration membranes with opposite surface charges for acidic wastewater treatment. Sep. Purif. Technol. 250, 117245. https://doi.org/10.1016/j.seppur.2020.117245.

Zhang, Y., Guo, M., Pan, G., Yan, H., Xu, J., Shi, Y., Shi, H., Liu, Y., 2015. Preparation and properties of novel pH-stable TFC membrane based on organic–inorganic hybrid composite materials for nanofiltration. J. Memb. Sci 476, 500–507. https://doi.org/10.1016/j.memsci.2014.12.011.

Zhang, Y., Guo, M., Yan, H., Pan, G., Xu, J., Shi, Y., Liu, Y., 2014. Novel organic–inorganic hybrid composite membranes for nanofiltration of acid and alkaline media. RSC. Adv. 4, 57522–57528. https://doi.org/10.1039/C4RA09090J.

Zhang, Y., Guo, Y., Wan, Y., Pan, G., Yu, H., Du, W., Shi, H., Zhao, M., Zhao, G., Wu, C., Liu, Y., 2022. Tailoring molecular structure in the active layer of thin-film composite membrane for extreme pH condition. J. Polymer Res. 29, 308. https://doi.org/10.1007/s10965-022-03155-7.

Zhang, Y., Wan, Y., Li, Y., Pan, G., Yu, H., Du, W., Shi, H., Wu, C., Liu, Y., 2021. Thin-film composite nanofiltration membrane based on polyurea for extreme pH condition. J Memb. Sci. 635, 119472. https://doi.org/10.1016/j.memsci.2021.119472.

Zhao, G., Zhang, Y., Liu, Y., 2023. pH stable thin film composite poly(amine-urea) nanofiltration membranes with excellent rejection performance. Sep. Purif. Technol. 320, 124108. https://doi.org/10.1016/j.seppur.2023.124108.

Zhao, L., Xia, W., 2009. Stainless steel membrane UF coupled with NF process for the recovery of sodium hydroxide from alkaline wastewater in chitin processing. Desalination. 249, 774–780. https://doi.org/10.1016/j.desal.2009.01.036.

Zhu, A., Long, F., Wang, X., Zhu, W., Ma, J., 2007. The negative rejection of H+ in NF of carbonate solution and its influences on membrane performance. Chemosphere 67, 1558–1565. https://doi.org/10.1016/j.chemosphere.2006.11.065.